Michigan State University

National Superconducting Cyclotron Laboratory

COULOMB INSTABILITIES AND MULTIFRAGMENT DECAYS

M. D'AGOSTINO, G. J KUNDE, P. M. MILAZZO, J. D. DINIUS, M. BRUNO, N. COLONNA, M. L. FIANDRI, C. K. GELBKE, T. GLASMACHER, F. GRAMEGNA, D. O. HANDZY, W. C. HSI, M. HUANG, M. A. LISA, W. G. LYNCH, P. F. MASTINU, C. P. MONTOYA, A. MORONI, G. F. PEASLEE, L. PHAIR, R. RUI, C. SCHWARZ, M. B. TSANG, G. VANNINI, and C. WILLIAMS

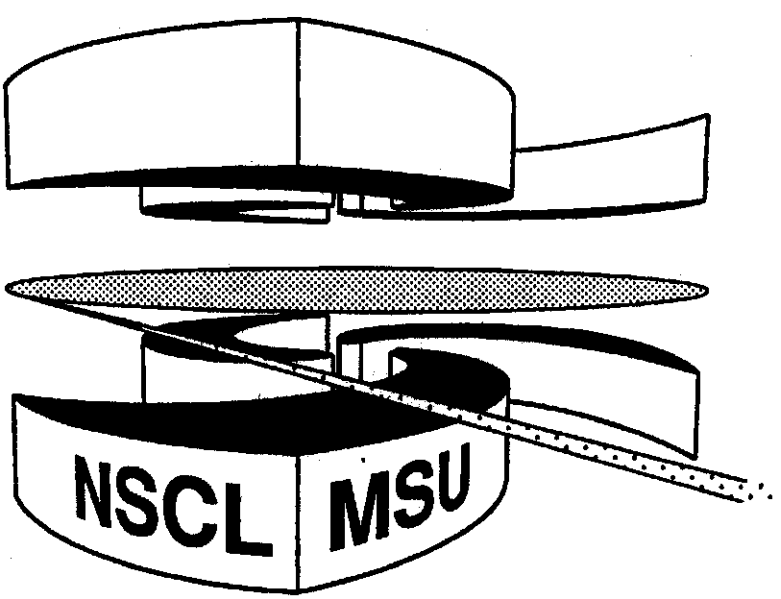

MSUCL-975

JULY 1995

Coulomb Instabilities and Multifragment Decays

M. D'Agostino[2], G. J. Kunde[6], P. M. Milazzo[2], J. D. Dinius[6], M. Bruno[2], N. Colonna', M. L. Fiandri[2], C. K. Gelbkes, T. Glasmacher[6], F. Gramegna[3], D. 0. Handzy[6], W. C. Hsi[6], M. Huang [6], M. A. Lisa[6 a], W. G. Lynch[6], P. F. Mastinu[2], C. P. Montoya[6 b], A. Moroni[4], G. F. Peaslee[6 c], L. Phaire [a], R.. Rui[5], C. Schwarz[6 d], M. B. Tsang[6], G. Vannini[5], and C. Williams[6]

[1] *INFN, Via Amendola 179, 70126 Bari, Italy*

[2] *Dipartimento di Fisica and ZNFN, Via Irnerio 46, 40126 Bologna, Ztaly*

[3] *ZNFN, Laboratori Nazionali di Legnaro, Via Romea 4, 85020 Legnaro, Italy*

[4] *ZNFN, Via Celoria 12, 20133 Milano, Italy*

[5] *Dipartimento di Fisica and ZNFN, Via Valerio 2, 34127 Trieste, Italy*

[6] *NSCL and Department of Physics and Astronomy, Michigan State University, East Lansing, MI 48824, USA*

Abstract

Multifragment disintegrations have been measured for central Au+Au collisions at $E/A = 35$ MeV. Fragment emission occurs predominantly at low center of mass energies of about $E/A \approx 5$ MeV, consistent with a Coulomb dominated breakup of a single source. Mean fragment multiplicities of $< N_{IMF} > \approx$ 10.8 are extracted after correction for the detection efficiency. The fragment charge distributions decrease much more gradually than expected from scaling laws recently applied to the extraction of critical exponents for the nuclear liquid-gas phase transition from nuclear collisions.

PACS number: 25.70Pq, 25.70Gh

Very highly charged nuclear systems are fundamentally unstable. At low excitation energies this instability manifests itself by the binary fission of heavy ($Z > 90$) nuclei [1], and at higher excitation energies, by the binary disintegration of highly charged systems ($184 \geq Z \geq 92$) formed momentarily in central, near Coulomb barrier collisions [2]. Coulomb [3] and isospin effects [4] are also predicted to strongly modify the characteristics of low density phase transitions in nuclear matter, and to significantly alter the collision dynamics, increasing the likelyhood of a multifragment disintegration [5,6,8,7]. The predicted consequences of Coulomb instabilities include the formation of bubble-like multifragment breakup configurations in central collisions at $E_{beam}/A \approx 30$ MeV [8] , and a monotonic increase in the fragment admixtures with decreasing excitiation energy [5,6]. If true, this latter prediction could obviate present techniques for the extraction of critical exponents from fragment charge distributions [9–11] and complicate the extrapolation of present measurements of the limit of infinite nuclear matter [6].

Even though the Coulomb interaction is known to strongly modify nuclear properties, little is experimentally known about Coulomb driven multifragment decays. Collisions between highly charged Au nuclei at incident energies of $E/A = 100$ MeV, are characterized by a very large collective expansion of the compressed central region formed during the early stages of the collision [12,13]. For such violent collisions, Coulomb instabilities may play only a minor role. A few measurements of the multifragment disintegration of very highly charged systems ($Z_{tot} \geq 130$) have been performed at low incident energies ($E/A \approx 30$ MeV) which suggest that bulk multifragmentation processes contribute little to a total reaction cross section dominated by strongly damped binary collisions [14,15]. In this letter, we present measurement of very central Au+Au collisions at a slightly higher energy, $E/A = 35$ MeV which strongly suggest a Coulomb driven multifragment decay. Consistent with recent molecular dynamics calculations of highly charged systems [5], we observe remarkably flat elemental distributions that are predicted to be a consequence of the destabilizing Coulomb interaction and are inconsistent with the assumptions of recent extractions of critical exponents for the nuclear liquid-gas phase transition [9–11].

The experiment was performed at the National Superconducting Cyclotron Laboratory of Michigan State University. Beams of Au ions at $E/A = 35$ MeV incident energy, accelerated by the K1200 cyclotron, were used to bombard Au foils of approximately 5 mg/cm^2 areal density. Light charged particles and intermediate mass fragments (IMF's: $3 \leq Z_{\rm IMF} \leq 20$) were detected at $23° \leq \Theta_{lab} \leq 160°$ by 158 phoswich detector elements of the MSU Miniball [16] and fragments with $3 \leq Z \leq 79$ at $3° \leq \Theta_{lab} \leq 23°$ by 44 gas-Si-Si(Li)-CsI detectors of the INFN Multics Array [17]. The charge identification thresholds were about 2, 3, and 4 MeV/nucleon in the Miniball for Z=3, 10, and 18, respectively, and about 1.5 MeV/nucleon in the Multics Array independent of fragment charge. To achieve higher precision in the Miniball energy calibrations, however, a higher energy threshold of E/A = 5 MeV was imposed upon the analysis of particles detected in the miniball. The geometric acceptance of the combined array was greater than 87% of 4π.

For the analysis reported here, impact parameters were selected via constraints upon the total charged–particle multiplicity detected in the combined system. Assuming that the charged–particle multiplicity decreases monotonically with impact parameter, a "reduced" impact parameter, $\hat{b} = b/b_{\rm max}$, for each event was determined according to [18]

$$\hat{b} = \frac{b}{b_{\rm max}} = \left[\int_{N_C(b)}^{\infty} dN_C \cdot P\left(N_C\right) \right]^{1/2} , \qquad (1)$$

Here, $P\left(N_C\right)$ is the probability distribution for the charged–particle multiplicity for N_C >2, and $\pi b_{\rm max}^2$ is the cross section for collisions with $N_C > 2$.

The analysis focused upon central events with $N_c \geq 28$ corresponding to $\hat{b} \leq 0.1$. For such events, approximately 53% of the total charge is detected in the experimental apparatus, and a surprisingly large fraction, 58%, of this detected charge is bound in intermediate mass fragments IMF's, defined here by $3 \leq Z_{\rm IMF} \leq 20$. Using the inherent symmetry of the Au+Au reaction [19], the detection efficiency was determined and an efficiency corrected mean IMF multiplicity $< N_{\rm IMF} >= 10.8 \pm 1$ was obtained. The corresponding efficiency corrected charge distribution, shown by the solid points in Fig. 1, is surprisingly flat. A

similarly flat charge distribution, shown by the open points, is also observed for fragments emitted at center of mass angles of $\theta_{\rm c.m.} = 90° \pm 20°$ suggesting that the large abundance of heavier fragments do not originate from the decay of projectile- and target-like remnants. (Differences between the two sets of data are comparable to the systematic uncertainties in the efficiency correction.) For comparison, we show the charge distribution measured for central collisions at E/A = 100 MeV (solid squares) for the same system [20] , and the charge distribution measured in peripheral collisions at E/A = 1000 MeV for the same system (open squares) [20]. Both of these charge distributions measured at higher energies decrease much more steeply with fragment charge.

Early investigations of high-energy hadron-nucleus collisions, revealed a power-law behavior, $p(A) \propto A^{-\tau}$, of the inclusive mass distributions [21], similar to that observed for the distributions of droplets for near-critical, macroscopic systems exhibiting a liquid and a gaseous phase [22]. Consistent with this macroscopic analogy, values for the "critical parameter" of τ have been extracted [9,10] from analyses of charge distributions measured for smaller systems containing 80-200 nucleons. After correction for finite size effects and detection efficiency values for $\tau \approx 2.2$ are obtained for peripheral collisions in the domain of limiting fragmentation; one such example is provided by the data for slowly expanding systems produced via peripheral collisions at E/A = 1000 MeV shown in Fig. 1. Similar data have been interpreted [9–11] as evidence for near critical behavior.

Such attempts to extract critical exponents [9–11] from scaling laws have relied heavily upon the assumption that the charge or mass distributions of systems at thermal equilibrium display minimum values for τ at the critical point. The charge distribution in Fig. 1 for E/A = 35 MeV can be described in the range of $3 \leq Z \leq 20$ by a χ^2-fit of a powerlaw with values for τ of $\tau = 1.22 \pm 0.05$. This value is much smaller than the value $\tau \approx 2.2$ expected from scaling laws at the critical point of the liquid gas phase diagram. Compared to this difference, finite size corrections to τ, deduced from percolation model calculations for systems with $A \approx 400$ [10], are negligible. This prompts more detailed consideration of other factors that could enhance the production of heavier fragments.

Angular momentum [23,24], Coulomb interactions [3,25] , non-equilibrium effects [26], and non-compact decay configurations [27] have been raised previously as important issues but have not been taken into account during the extraction [9–11] of critical exponents. Before focusing upon Coulomb effects, it is worthwhile considering some of these other possibilities. In particular, the selection of events with impact parameters $\hat{b} \leq 0.1$ used in the construction of Fig. 1 could imply nonnegligible total angular momenta and possible contributions from strongly damped reactions, due to the finite resolution of the impact parameter filter. One may assess the importance of the statistical decay of rapidly rotating projectile- and target-like residues with enhanced branching ratios for fragment emission [23,24,28] by examining the fragment velocity distributions, shown as a typical example for Z=7 in Figure 2 for peripheral ($\hat{b} \geq 0.7$; upper panel) and central collisions ($\hat{b} \leq 0.1$; lower panel), respectively [19]. Distributions of IMFs for peripheral and central collisions both have a major component centered about the center of mass velocity $v_{\rm c.m.}$; ring-like emission patterns, centered about the projectile- and target-like residue velocities and characteristic of the statistical decay of projectile- and target-like residues, are only weakly observed. Consistent with previous observations [29], fragments are primarily formed in peripheral collisions by the fragmentation of a "neck" that momentarily connects projectile and target-like residues. This "neck" forms a "participant" source that grows in size and importance with decreasing impact parameter until it encompasses the entire system. The assumption of a constant *rms* fragment velocity of $v_{rms} = (< v^2_{\rm c.m.} >)^{1/2} \approx 0.1$ c, extracted for fragments emitted in central collisions at $70° \leq \Theta_{\rm c.m.} \leq 110°$ and shown as the circle in Fig. 2, is approximately correct for the participant source at other angles [30]. Such a low value for v_{rms} is roughly consistent with the Coulomb disintegration of a single spherical source at a constant density of about $0.25 - 0.3\rho_0$. This conclusion is supported by other more detailed investigations of single and multifragment observables [30].

While the statistical decay of equilibrated projectile- and target-like residues or of an equilibrated compound nucleus is unlikely for central collisions, it is possible, that for a phase space dominated decay mechanism, collective rotation could dictate large branching ratios

for non-compound fragment emission [23,24,28]. Since such general considerations would also dictate the focusing of decay patterns into the plane perpendicular to the total angular momentum [28,31], the importance of collective rotation can be tested by constructing $\alpha-\alpha$ azimuthal angular correlation functions $1 + R(\Delta\phi_{\alpha\alpha})$, defined by

$$\sum Y_{12}(\vec{p}_1, \vec{p}_2) = [1 + R(\Delta\phi_{\alpha\alpha})] \cdot \sum Y_1(\vec{p}_1) \cdot Y_2(\vec{p}_2). \quad (2)$$

Here, $Y_{12}(\vec{p}_1, \vec{p}_2)$ is the coincidence yield, $Y_1(\vec{p}_1)$ and $Y_2(\vec{p}_2)$ are the singles yields for the particles 1 and 2 at momenta $\vec{p}_1$ and $\vec{p}_2$, and $\Delta\phi_{\alpha\alpha} = \phi_{\alpha_1} - \phi_{\alpha_2}$ is the relative azimuthal angle between the two alpha particles about the beam axis. Both sides of Eq. 2 are summed over momenta $\vec{p}_1$ and $\vec{p}_2$, for fixed $\Delta\phi_{\alpha\alpha}$. For systems rotating collectively, emission occurs preferentially at relative azimuthal angles of $\phi_{\alpha\alpha} = 0°$ and $180°$ corresponding to coplanar emission of the α particles in directions perpendicular to the total angular momentum.

Impact parameter selected correlation functions are shown in Figure 3 for an energy gate of $E_{\text{c.m.}}/A \geq 7$MeV and an angular gate of $70° \leq \Theta_{\text{c.m.}} \leq 110°$. Correlation functions for larger impact parameter collisions, $0.7 \leq \hat{b} \leq 1.0$, display large azimuthal anisotropies consistent with either a collective rotation of such residues or significant refractive "rotational" flow of nucleons along the surfaces of the combined system. In contrast, correlation functions of central collisions $\hat{b} \leq 0.1$ are nearly isotropic, indicating that anisotropies induced by rotational effects are comparatively negligible at such small impact parameters. No strong preference for the alignment of the angular momenta of the two alpha particles parallel to the total angular momentum is observed. This strongly suggests that the influence of rotation upon the fragment charge distributions will likewise be small.

There are a number of theoretical investigations that predict the observation of unusually flat fragment charge distributions. Reduced values of the extracted "effective" critical parameter $\tau \approx 1.7$ have been attributed to the existence of a non-equilibrium mixture of fragments and a supersaturated nucleonic gas at freezeout [9]. Within microcanonical fragmentation models [3,25], the Coulomb interaction causes significantly larger fragment admixtures [3] and a preference for bubble-like fragment spacial distributions [25]. Within

bond percolation models [27], such non-compact bubble-like decay configurations can display values for the critical parameter τ that are 20% smaller than those for compact spherical systems. Classical molecular dynamical simulations of neutral, initially thermalized liquid drops predict a non-equilibrium fragmentation within the region of adiabatic instability [26,7], and a reduction in the effective critical exponent τ in heavy systems to values of about $\tau \approx 1.6$. Only when the Coulomb interaction is introduced, however, do the τ values for the multifragment decay configurations of the molecular dynamics calculations decrease monotonically as the excitation energy is lowered and attain values of order unity as experimentally observed [5,6]. Thus the available information suggests that the most likely cause for the extreme flatness of the charge distribution is the destabilizing Coulomb interaction.

In summary, multifragment disintegrations have been measured for central Au+Au collisions at $E/A = 35$ MeV. Fragment emission occurs predominantly at low emission energies of about $E/A \approx 5$ MeV, consistent with a Coulomb dominated breakup of a single source. Mean intermediate mass fragment multiplicities of $< N_{\rm IMF} > \approx 10.8$ are extracted. Fragment charge distributions are observed that decrease much more gradually than would be consistent with recent extractions of critical exponents for the nuclear liquid-gas phase transition. These observations are qualitatively consistent with trends predicted for Coulomb driven multifragment decays of highly charged systems. Additional experimental and theoretical work is required to quantitatively understand the present observations.

This work was supported by the National Science Foundation under Grant Phy-92-14992. The authors are indebted to Prof. I. Iori for stimulating and constructive discussions and to P. Buttazzo, L. Celano, A. Ferrero, L. Manduci, G.V. Margagliotti, F. Petruzzelli, R. Scardaoni for the help during the measurements. The technical assistance of R. Bassini, C. Boiano, S. Brambilla, G. Busacchi, A. Cortesi, M. Malatesta is gratefully acknowledged. One of us, G.J.K. acknowledges the support from the Alexander-von-Humboldt foundation.

FIGURE 1

Efficiency corrected and angular integrated elemental probability distribution for fragments emitted in central collisions ($\hat{b} \leq 0.1$) for the reaction Au+Au at $E/A = 35$ MeV (solid points). The corresponding differential distribution at $\Theta_{\text{c.m.}} = 90° \pm 20°$, normalized to the angular integrated data, is shown as open points. Elemental yields for central collisions at $E/A = 100$ MeV and peripheral collisions at $E/A = 1000$ MeV from ref. [20] are normalized to the lithium yield at $E/A = 35$ MeV and are shown by the solid and open squares respectively.

FIGURE 2

Velocity distribution $\frac{dP}{dv_{\parallel}dv_{\perp}}$ for $Z = 7$ fragments emitted in peripheral collisions ($\hat{b} \geq 0.7$, upper panel) and central collisions ($\hat{b} \leq 0.1$, lower panel). The velocity axes are in units of the speed of light and the intensity scale is logarithmic. The circle corresponds to a fixed velocity of 0.1c in the center of mass. (In this figure, the efficiency corrected velocity distributions at $v \geq v_{\text{c.m.}}$ have been reflected about the center of mass velocity $v_{\text{c.m.}}$ to obtain a thresholdless distribution for all velocities.)

FIGURE 3

$\alpha - \alpha$ azimuthal correlation functions [32] for peripheral (open points) and central (solid points) collisions. The relevant energy and angular gates are given in the text.

REFERENCES

[a] Present address: Nuclear Science Division, Lawrence Berkeley Laboratory, Univ. of California, Berkeley CA 94720, USA

[b] Present address: Merrill Lynch, World Financial Center, North Tower, New York NY 10281, USA

[c] Present address: Physics Department, Hope College, Holland MI 49423, USA

[d] Present address: Gesellschaft für Schwerionenforschung, D-64220 Darmstadt, Germany

[1] Robert Vandenbosch and John R. Huizenga, Nuclear Fission, Academic Press (1973) and ref. therein.

[2] W.U. Schröder and J.R. Huizenga, Vol. 2 of Treatise on Heavy Ion Science, Plenum Press (1984) and refs. therein.

[3] D.H.E Gross et al., Nucl. Phys. **A545**, 187c (1992).

[4] H. Mueller et al., Indiana Univ. preprint NTC 95-04 (1995).

[5] S. Das Gupta and J. Pan, submitted to Phys. Rev. **C** (1995).

[6] G.J. Kunde et al., to be published (1995).

[7] A.Vincentini et at., Phys. Rev. **C 31**, 1783 (1985); R.J. Lenk et al. Phys. Rev. **C 34**, 177 (1986); T.J. Schlagel et al. Phys. Rev. **C 36**, 162 (1986).

[8] B. Borderie et al., Phys. Lett. **B 302**, 15 (1993).

[9] M. Mahi et al., Phys. Rev. Lett. **60**, 1936 (1988).

[10] T. Li et al., Phys. Rev. Lett. **70**, 1924 (1993).

[11] M.L. Gilkes et al., Phys. Rev. Lett. **73**, 590 (1994).

[12] S.G. Jeong et al., Phys. Rev. Lett. **72**, 3468 (1994).

[13] W.C. Hsi et al., Phys. Rev. Lett. **73**, 3367 (1994).

[14] J.F. Lecolley et al., Phys. Lett. **B 325**, 317 (1994).

[15] B. M. Quednau et al., Phys. Lett. **B 309**, 10 (1993).

[16] R.T. de Souza et al., Nucl. Instr. Meth. **A 295**, 109 (1990).

[17] I.Iori et al., Nucl. Instr. Meth. **A 325**, 458 (1993).

[18] C. Cavata et al., Phys. Rev. **C 42**, 1760 (1990); Y.D. Kim et al., Phys. Rev. **C 45**, 338 (1992).

[19] The detection efficiency $\varepsilon(\theta)$ could be accurately determined at $v \geq v_{c.m.}$ and $\theta_{lab} > 3°$ where it is purely geometric and not vanish. Both the efficiency corrected fragment yield and the efficiency corrected velocity distribution in Fig. 2 were therefore determined at $v \geq v_{c.m.}$ and reflected about $v = v_{c.m.}$ to obtain the values for $v \leq v_{c.m.}$.

[20] G.J. Kunde et al. Phys. Rev. Lett. **74**, 38 (1995).

[21] A.S. Hirsch et al., Phys. Rev. **C 29**, 508 (1984).

[22] M.E.Fisher, Physics **3**, 255 (1967).

[23] W.A. Friedman et al., Nucl. Phys. **A471**, 327c (1987).

[24] L.G. Sobotka et at. Nucl. Phys. **A471**, 111c (1987).

[25] D.H.E Gross et al. Nucl. Phys. **A567**, 317 (1994).

[26] S. Pratt et al., Phys. Lett. **B 349**, 261 (1995).

[27] L. Phair et al., Phys. Lett. **B 314**, 271 (1995).

[28] K. Sneppen et al., Nucl. Phys. **A480**, 342 (1988).

[29] C.P. Montoya et al. Phys. Rev. Lett. **73**, 3070 (1994).

[30] M. D'Agostino et al. submitted to Phys Lett. **B** (1995).

[31] T.E.O. Erikson et al., Nucl. Phys. **8**, 284 (1958); Nucl. Phys. **9**, 689 (1959).

[32] Rotational effects are responsible for the suppression of emission at $\Delta\phi \approx 90°$. Differences between the value of the $\alpha - \alpha$ correlation function at $\Delta\phi \approx 0°$ and 180° result from final state interactions between α-particles [33].

[33] J.Pochodzalla et al. Phys. Lett. **B 161**, 275 (1985).

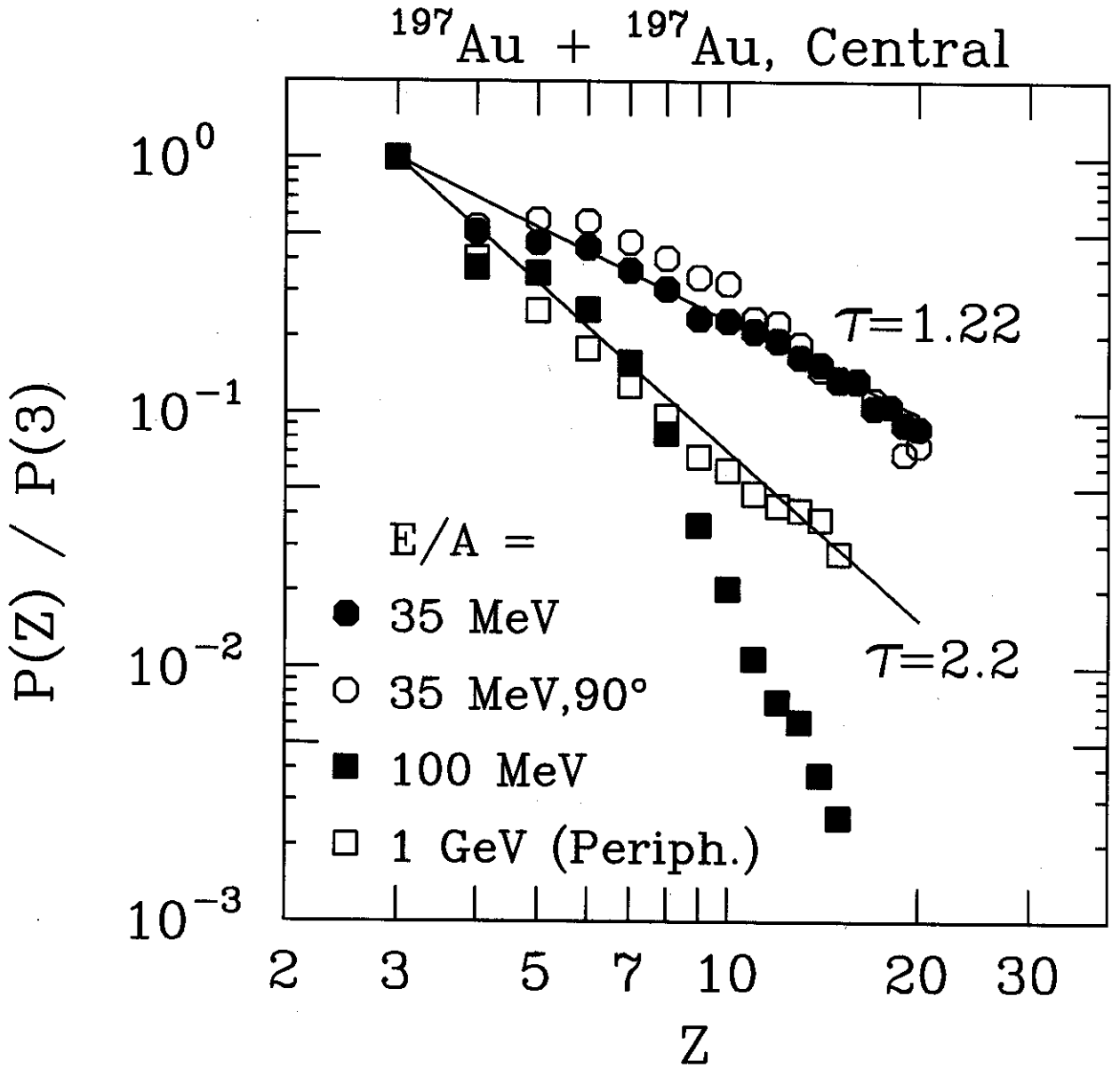
197Au + 197Au, Central
P(Z) / P(3)
10^0
10^-1
10^-2
10^-3
2
3
5
7
10
20
30
Z
τ=1.22
τ=2.2
E/A =
35 MeV
35 MeV,90°
100 MeV
1 GeV (Periph.)

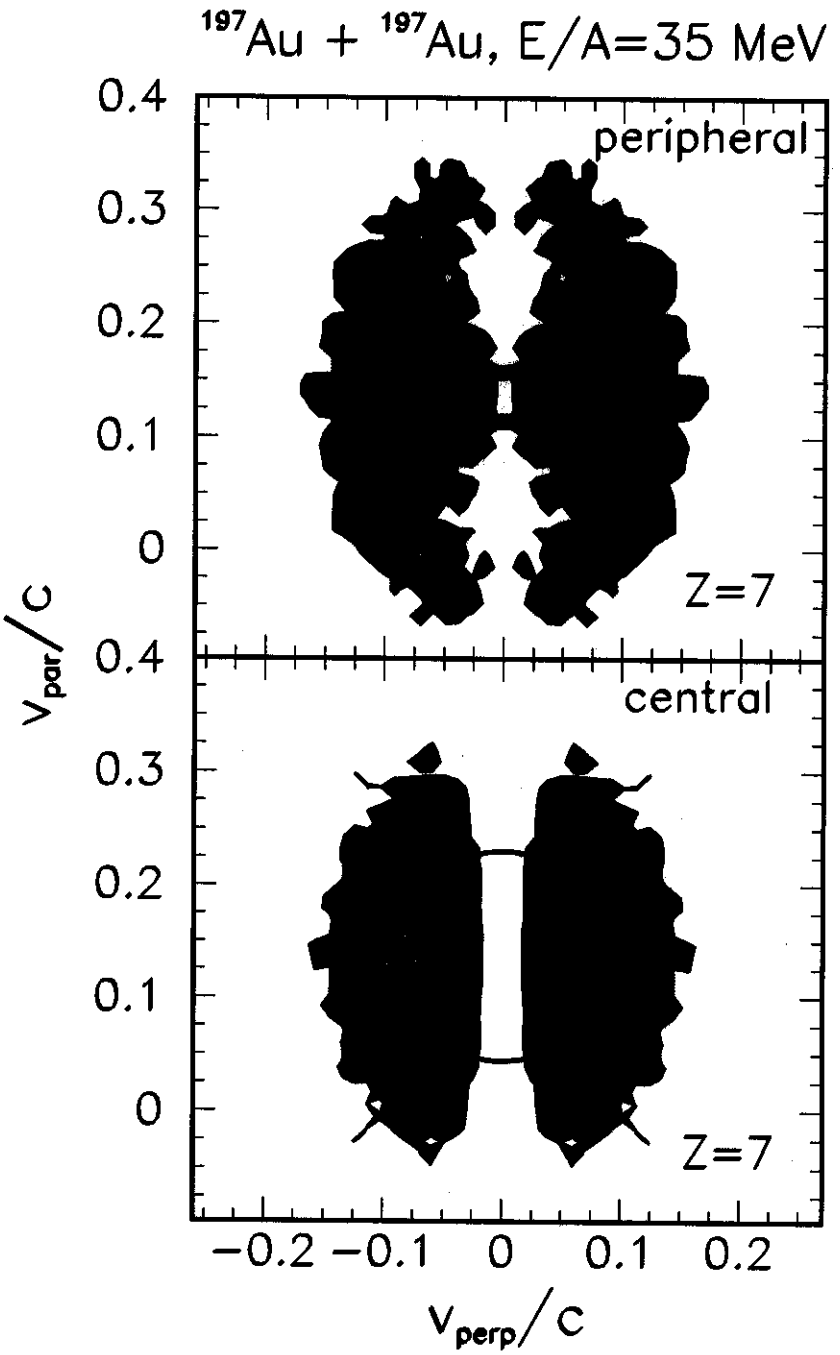
197Au + 197Au, E/A=35 MeV
peripheral
Z=7
central
Z=7
0.4
0.3
0.2
0.1
0
0.4
0.3
0.2
0.1
0
−0.2 −0.1 0 0.1 0.2
v_par/c
v_perp/c

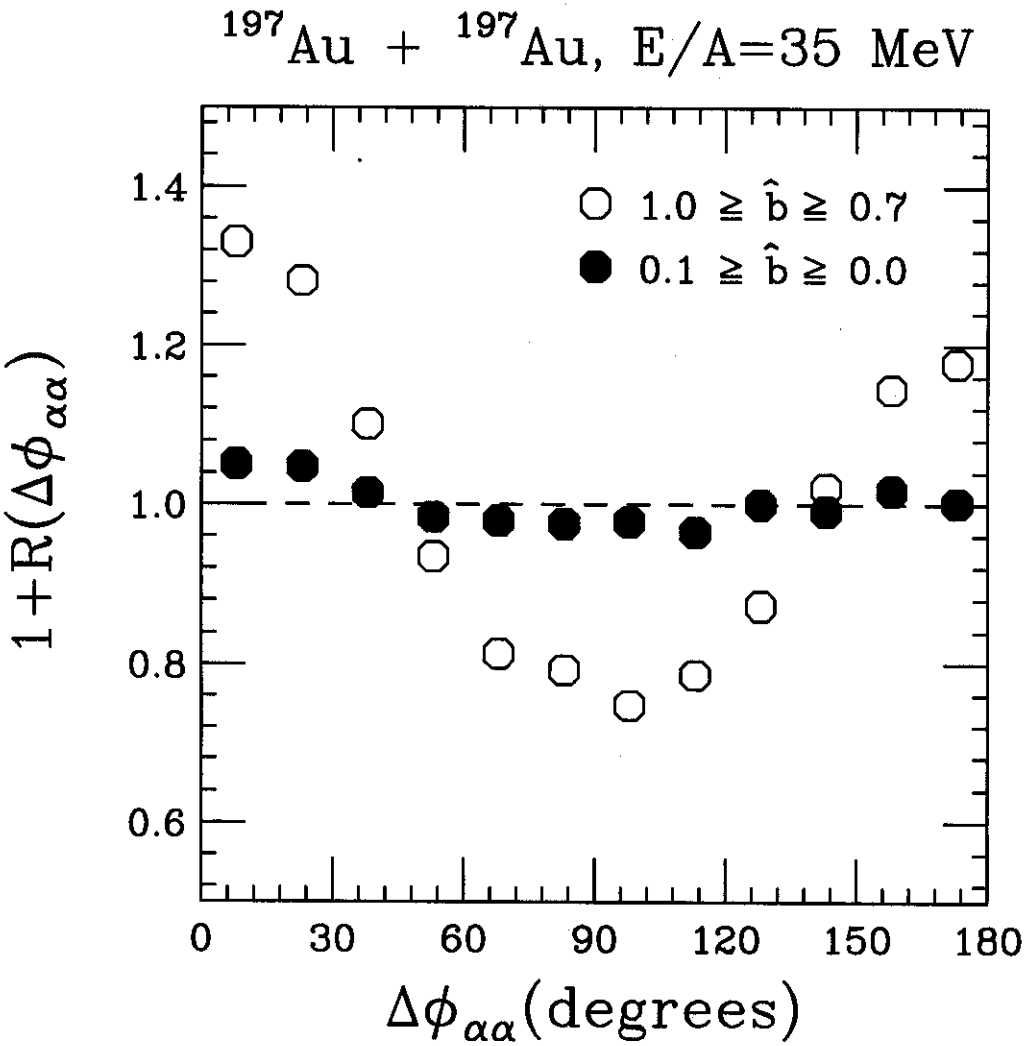
^{197}Au + ^{197}Au, E/A=35 MeV
1.0 ≧ b̂ ≧ 0.7
0.1 ≧ b̂ ≧ 0.0
1+R(Δφαα)
Δφαα(degrees)
0.6
0.8
1.0
1.2
1.4
0
30
60
90
120
150
180